

# MINERALOGICAL MAGAZINE

VOLUME 49

NUMBER 354

DECEMBER 1985

## The Tugtutôq older giant dyke complex: mineralogy and geochemistry of an alkali gabbro–augite–syenite–foyaite association in the Gardar Province of South Greenland

B. G. J. UPTON

Grant Institute of Geology, University of Edinburgh, Edinburgh EH9 3JW

D. STEPHENSON

British Geological Survey, Murchison House, Edinburgh EH9 3LA

AND

A. R. MARTIN

Grant Institute of Geology, University of Edinburgh, Edinburgh EH9 3JW

**ABSTRACT.** The Older Giant Dyke Complex is a differentiated alkaline intrusion of Proterozoic age ( $1154 \pm 16$  Ma) and is the earliest of the late Gardar intrusions in the Tugtutôq–Ilimaussaq region. The dyke is approximately 20 km long by 0.5 km broad and comprises (i) marginal 'border group' rocks of alkali olivine gabbro, grading inwards to ferro-syenogabbro and (ii) an axial 'central group' of salic rocks ranging from augite syenite in the WSW to sodalite foyaite in the ENE.

Chilled margins contain plagioclase ( $An_{53}$ ), olivine ( $Fo_{53}$ ), magnetite, ilmenite, and apatite as liquidus phases and later-crystallized augite ( $Di_{69}Hd_{27}Ac_4$ ) and biotite ( $Annite_{32}$ ). The coexisting Fe–Ti oxides indicate  $f_{O_2}$  and  $T$  values just below the synthetic QFM buffer curve. In the border group, plagioclase cores zone into anorthoclase and soda-sanidine rims, olivines reach  $Fo_{16}$ , pyroxenes  $Di_{32}Hd_{59}Ac_9$ , and biotites  $Annite_{86}$ . Interstitial pargasitic amphibole appears close to the innermost margins. In the central group, feldspars are all perthitic alkali feldspars and nepheline becomes a major, early crystallizing phase. Olivines range from  $Fo_{10}$ – $Fo_4$  in the augite-syenites where they coexist with ferro-salites  $Di_{50}Hd_{47}Ac_3$ , but olivine is absent from foyaitic assemblages in which the pyroxenes range through aegirine–augite to pure aegirine. Interstitial amphiboles range from ferro-pargasite or hastingsite to katophorite and thence

towards arfvedsonite, but are absent from the most differentiated rocks, whereas biotite occurs throughout the entire group in the range  $Annite_{71}$ – $Annite_{100}$ .

The parental magma, represented by the chilled margins, was a relatively anhydrous alkali olivine-basalt with an initial  $^{87}Sr/^{86}Sr$  ratio of 0.70326. Its high Ti, P, Ba, and F contents are inferred to be features inherited from a primary magma, derived from the mantle as a small partial melt fraction which involved significant amounts of fluor-apatite and phlogopite. While all lithologies are considered as differentiates from this parental magma, there is both a well-defined field junction and a compositional hiatus between the border group and the central group rocks. Mineralogical considerations and *REE* patterns suggest that the later, more salic (?benmoreitic) magma from which the central group crystallized, related to the parental magma by ol–fsp–ap–FeTi oxide fractionation. Congelation in both border group and central group occurred by side-wall crystallization, but the salic magma became compositionally stratified, with upward concentration of alkalis and volatiles to produce a phonolitic upper facies which is preserved at the ENE end of the intrusion owing to subsequent axial tilting.

**KEYWORDS:** mineralogy, geochemistry, alkali gabbro, foyaite, Gardar, Greenland.

THE alkaline igneous rocks of the Gardar province in southern Greenland were erupted during the interval 1350–1120 Ma in a region adjacent to, and overlapping, the southern margin of the Archaean craton (Emeleus and Upton, 1976; Blaxland *et al.*, 1978). Although the most abundant magmas within this intraplate continental province were mildly alkaline olivine basalts and hawaiites, with trachytic, phonolitic, and rhyolitic derivatives, the major intrusive complexes are mainly composed of coarse-grained products from the salic differentiates.

The petrology and mineralogy of the principal silica-undersaturated salic complexes has been studied in considerable detail (Gill, 1972; Stephenson, 1972, 1974, 1976; Chambers, 1976; Larsen, 1976; Powell, 1978; Jones, 1980, 1984). Their main components are augite-syenite, pulaskite, foyaite, with more extreme agpaite lithologies present in the Ilímaussaq and Motzfeldt Complexes. There is general consensus that the salic rocks are largely related to an augite-syenite (benmoreite-trachyte) parental magma. Although gabbroic or syenogabbroic units occur as minor, late constituents in the Motzfeldt and Igdlerfigssalik complexes, rocks more basic than augite-syenite are generally absent.

The Older Giant Dyke Complex (OGDC) on Tugtutôq, formerly referred to as the Hviddal intrusion (Upton, 1962; 1964*a, b*), is of particular interest and relevance to the genesis of these large undersaturated complexes. Individual intrusive

units of the larger Gardar foyaitic complexes commonly display little compositional variation within themselves and the genetic relationship of one unit to another is often a matter of conjecture. By contrast, the OGDC not only shows a wider compositional range, from relatively primitive olivine gabbro to peralkaline sodalite foyaite, but displays gradational relationships within this suite except for a minor compositional hiatus between syenogabbro and augite-syenite.

#### *Field-setting*

Late Gardar (*c.*1150 Ma) extensional tectonics gave rise to an abundance of predominantly doleritic/gabbroic dykes within two near-parallel ENE–WSW zones running through (i) the Nunarsuit–Isortôq and (ii) the Tugtutôq–Narssarsuaq areas respectively (Upton and Blundell, 1978). In both zones there was a tendency for salic central-type complexes to post-date the main phases of dyke emplacement. The swarms include a number of exceptionally broad dykes (giant dykes) with widths up to 0.8 km (Emeleus and Upton, 1976). The OGDC, with a width of 0.5–0.6 km and outcrop length of some 20 km is one such giant dyke and is the earliest of the late Gardar intrusions in the Tugtutôq region (fig. 1). For much of its length it is composite, consisting of mafic rocks in zones up to 100 m broad on either side of the dyke

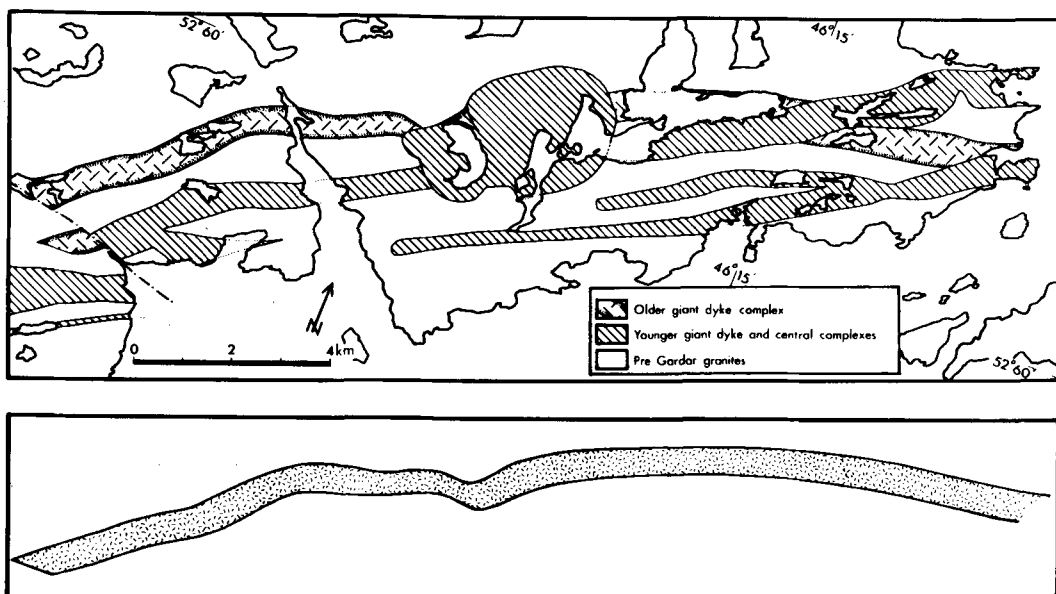


FIG. 1. (Upper) Geological sketch map of Tugtutôq showing the OGDC and the cross-cutting YGDC and central complex. (Lower) Reconstructed map of the OGDC prior to faulting and later intrusions.

and a younger salic unit forming the central portion. The mafic rocks range from fine-grained, well-chilled olivine gabbros at their outer contacts, to coarse-grained syenogabbroic facies at their inner margins. Whereas the composition of these mafic rocks (border group) appears to be essentially unchanged along the length of the dyke, the axial salic unit grades from augite-syenite at the western end, through pulaskitic varieties, to peralkaline sodalite foyaites at the eastern extremity.

Emplacement of the OGDC was followed by intrusion of two further giant dykes, which traverse Tugtutôq and its south-western archipelago. The term Younger Giant Dyke Complex (YGDC) has been used to describe collectively these later giant dykes, their offshoots and a larger gabbroic body on the mainland to the east at Narssaq (Upton and Thomas, 1980). The YGDC is largely composed of olivine gabbro but locally also exhibits a composite character where more differentiated rocks occur as broad axial units. However, whereas the OGDC only involves undersaturated rocks, the YGDC gave rise to quartz syenites and peralkaline granites. Both dyke complexes were subsequently affected by a left-lateral fault trending  $c.100^\circ$  with a displacement of  $c.2.4$  km. Further disturbance to the giant dykes occurred when they were intersected by the quartz syenites and alkaline granites of the Central Tugtutôq Complex. The present field-relationship is shown in fig. 1 together with a reconstruction of the OGDC as envisaged prior to faulting and the later intrusions.

The country-rocks to the Tugtutôq giant dykes are the granodiorites and tonalites of the Julianeåb Granite complex, dated at approximately 1600 Ma (van Breemen *et al.*, 1974). However, the early Gardar sandstones and lavas of the Eriksfjord Formation which are preserved to the east of Tugtutôq, unconformably overlie the Julianeåb Granite and must have extended over much of the Tugtutôq region in late Gardar times (Upton, 1962). Although the Eriksfjord Formation is now only some 3 km thick, the sequence at the time of the giant dyke intrusions is likely to have been substantially thicker (Jones, 1980).

Upton (1962) considered the OGDC to be a composite dyke in the classic sense, formed by two successive inputs of magma, first basic and then salic. Subsequently, it was suggested that only a single magmatic filling may have been involved (Emeleus and Upton, 1976): on this supposition, the augite-syenites, pulaskites, and foyaites of the dyke centre are predominantly cumulates, developed at a late-stage overlying an unexposed stack of syenogabbro and gabbro cumulates, enclosed between border groups of basic rocks that had accreted inwards from the walls. In both (single- and

composite-) models, the lateral variation of the salic rocks along the dyke centre is explicable if the dyke is regarded as a layered intrusion that has been tilted down towards the east about an axis quasi-perpendicular to the dyke walls, and eroded so as to reveal lower levels in the WSW and successively higher levels towards the ENE. It was proposed that the exposed syenitic rocks could represent a series of cumulates approximately 2 km thick (Upton, 1964b). However, re-examination of the dyke complex has called for modification of this hypothesis. The salic (central-group) rocks lack the low-angle layering (feldspar lamination, rhythmic layering, etc.) that might have been expected to accompany the supposed cryptic layering, whereas, on the contrary, they do show occasional signs of near-vertical mafic layering, generally parallel to the dyke walls (fig. 2). Whereas the concept of an axially tilted dyke, allowing access to structurally higher levels to the east, is retained, it appears that crystallization of both the border-group rocks and the central-group rocks took place from the margins inwards and that the idea of the central-group having originated as low-angle crystal cumulates built up from some kind of 'floor' in the dyke interior, should be abandoned.



FIG. 2. Crumbly outcrops of sodalite foyaites at the eastern end of the OGDC outcrop. The Dyrnaes-Narssaq and Ilimaussaq complexes compose the mountainous region in the background. Weakly defined, steep-angled mafic layering can be discerned in the foyaites.

A gravity-survey demonstrated the presence of a linear 'gravity high' some 25 km broad and 80 km long, aligned WSW-ENE and centred on Tugtutôq (Blundell, 1978). This gravity anomaly, with an amplitude of over 300 g.u., was attributed to an underlying mass of high-density material intrusive into the crust and reaching close to the surface in an area coinciding with the Narssaq Gabbro, but



FIG. 3. Vertical 'pipe-structures' in augite-syenite, defined by near-vertical mafic layering.

which mostly lies at a depth of 3–5 km and extends down to 10 km. It has an estimated width of 30 km and is believed to lie at increasing depth as traced WSW from Narssaq (Blundell, 1978). The axial correspondence of the giant dykes with this 'gravity high' suggests that the latter are high-level offshoots from a very much greater mass of mafic rocks at depth.

The nature of the upper termination of the OGDC must remain speculative. However, by analogy with the roof zone of the YGDC and the behaviour of a giant dyke in the Motzfeldt Complex to the east (Jones, 1980), it is likely that the OGDC terminated bluntly or in a sill-like manner at, or about, the plane of unconformity separating the Julianehåb Granite from the Eriksfjord Formation. Fig. 4 depicts a schematic cross-section of the OGDC with a hypothetical sill-like top.

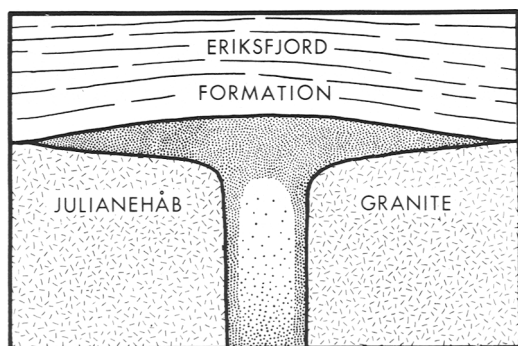


FIG. 4. Diagrammatic cross-section of the OGDC as it may have been prior to erosion. Section shows Eriksfjord Formation supracrustal strata overlying Julianehåb Granite intruded by the OGDC. Close-stipple: Border-group mafic rocks. Open-stipple: Central-group salic rocks grading up from augite-syenites to foyaites.

The OGDC is generally poorly exposed in relatively low ground (figs. 5 and 6). Its transverse structure is best seen along the coasts of a fjord which traverses the intrusion towards its western end. It is one of the few localities where chilled marginal samples can be obtained and the only place where the transition from the basic border-group to the salic central-group can be observed. The transition takes place over 2 or 3 m; it is manifested by a rapid lowering of the colour index and a change in the pyroxenes from ophitic to prismatic as one passes from syenogabbro to syenite. The syenogabbro close to the syenite contains prominent veins of pegmatitic feldspathoidal syenite. The central-group syenite shows no tendency to become finer-grained against the syenogabbro which was presumably still at a high temperature when the syenites commenced crystallization.



FIG. 5. View ENE along the OGDC, from the Tugtutôq Central Complex (foreground) to the Dyrnaes-Narssaq and Ilimaussaq Complexes (left, background). The OGDC underlies most of the lake in the mid-distance, outcrops being restricted in this sector, to small islands and lake shores.

From their abundant presence as xenoliths within many of the Gardar intrusions in the vicinity of the OGDC, anorthositic cumulates are believed to be a major rock-type at depth below the Tugtutôq area. Although anorthosite xenoliths and plagioclase megacrysts are abundant in the higher (i.e. more easterly) sectors of the YGDC they appear to be absent from the OGDC.

#### *Petrography*

The mafic border-group rocks are composed of feldspar (plagioclase zoned to alkali feldspar) olivine, augite, biotite, Ti-magnetite, ilmenite,

apatite, and micaceous pseudomorphs apparently after nepheline. Chalcopyrite and pyrrhotite occur as minor accessories. The ratio of alkali feldspar to plagioclase tends to increase from the chilled margins inwards. Similarly the ratio of augite (ophitic) to olivine (idiomorphic) rises inwards from the contacts and some pargasitic amphibole appears.



FIG. 6. View west along the OGDC from the fjord section across the western part of the intrusion. The valley is floored by augite-syenites with border-group basic rocks forming the rising ground towards the feet of the precipitous walls of Julianehåb Granite.

The augite-syenites composing the central group of the western third of the intrusion are mesocratic rocks with grain size up to c.6 mm, with white alkali feldspar and clusters of ferromagnesian minerals and apatite. The feldspars lack plagioclase cores and consist of crypto- and micro-perthite. The ferromagnesian clusters contain idiomorphic prisms of zoned clinopyroxene which are generally enclosed by amphibole. Fayalitic olivine commonly has outer fringes and inner lamellae of magnetite. The olivine-oxide aggregates are usually enclosed by blue-green amphibole which in turn is surrounded by biotite fringes. Nepheline, usually pseudomorphed by micas, occurs interstitially.

In the central group traced eastwards, olivine becomes increasingly scarce and is lost east of the contact with the central Tugtutôq complex, whereas the pyroxene becomes increasingly Fe- and Na-rich. Amphibole becomes progressively more scarce and disappears east of the central complex leaving aegirine and Ti-magnetite as the sole ferromagnesian minerals together with trace amounts of apatite. The alkali feldspars change in habit, becoming increasingly tabular (parallel to {010}) eastwards and the amount of feldspathoidal component increases. In the easternmost sector of

the dyke nepheline appears as squat idiomorphic prisms, commonly altered in part or in whole to 'gieseckite', sodalite, analcime, cancrinite, natrolite, and other zeolites. Pegmatitic patches, composed essentially of perthitic feldspar and aegirine, become prominent among the easternmost foyaitic syenites.

#### *Analytical techniques*

Mineral analyses were made on a Cambridge Scientific Instruments Microscan 5 electron-probe microanalyser at Edinburgh University, using either wavelength- or energy-dispersive methods. In all cases the standards used were of pure elements, oxides, or simple silicate compositions. Corrections were made for dead-time, atomic number, absorption, and fluorescence, using computer programs based on the methods of Sweatman and Long (1969).

The rock analyses were made at Edinburgh University using a Philips PW1450 XRF system. Major elements were determined on fused glass discs (Norrish and Hutton, 1969) with corrections applied for inter-element mass absorption effects. Trace elements were determined using pressed powder discs and corrected for mass absorption effects with coefficients calculated from the major element analyses. USGS and CRPG rock standards (Abbey, 1980) were used in the calibration of both major and trace elements. The precision and accuracy of the methods used have been described by Thirlwall (1979).

REE determinations were made at King's College, London, on twenty-six representative samples, using inductively coupled plasma spectrometry techniques on concentrated lanthanide solutions separated by cation exchange techniques (modified after Walsh *et al.*, 1981).

#### *Mineralogy*

Microprobe analyses were made of the ferromagnesian minerals and 'homogeneous' feldspars (plagioclases and cryptoperthites). No new data are presented for the exsolved feldspars, feldspathoids, or zeolites. Representative analyses of olivines, pyroxenes, biotites, and amphiboles are presented in Table I.

The overall trends and limits of major compositional variation in most mineral phases are closely similar to those obtained from other Gardar Si-undersaturated suites (Gill, 1972; Stephenson, 1972, 1974, 1976; Chambers, 1976; Larsen, 1976; Powell, 1978; Jones, 1980, 1984). Some phases (e.g. pyroxene, amphibole, and apatite) exhibit trends which differ significantly from those of most Si-oversaturated suites. Such contrasting trends are described by Stephenson and Upton (1982) and further elaboration is unnecessary in the present description.

*Feldspars* (34 analyses). Rocks of the border group contain feldspars which usually show intense zoning from cores of twinned plagioclase to clear, untwinned rims of alkali feldspar. Inner parts of the

Table I. Representative analyses of mafic silicates from the Tugtutøq Older Giant Dyke Complex.

	1	2	3	4	5	6	7	8	9	10	11
SiO <sub>2</sub>	35.23	29.40	50.43	49.45	49.75	50.96	37.87	39.94	43.98	36.70	33.97
TiO <sub>2</sub>	-	-	1.47	0.69	0.30	0.94	3.53	2.09	1.38	6.29	3.20
Al <sub>2</sub> O <sub>3</sub>	0.06	0.03	3.25	1.29	0.84	0.86	11.24	7.44	4.51	13.67	9.13
Fe <sub>2</sub> O <sub>3</sub> *	-	-	2.01	2.11	14.35	30.33	-	-	-	-	-
FeO	39.34	65.37	7.63	20.39	13.51	1.07	23.95	31.54	31.65	14.19	37.56
MnO	0.81	2.90	0.14	0.43	0.94	0.56	0.38	0.70	1.31	0.06	1.18
MgO	24.58	1.85	12.17	3.94	1.10	0.36	4.92	1.43	1.39	13.87	0.92
CaO	0.26	0.56	22.18	21.47	13.69	4.46	10.89	8.68	4.87	-	0.09
Na <sub>2</sub> O	-	-	0.78	0.82	5.57	11.77	2.64	3.87	6.06	0.21	0.44
K <sub>2</sub> O	-	-	-	-	-	-	1.61	1.64	1.66	9.64	8.11
F	-	-	-	-	-	-	0.24	0.19	0.73	0.34	0.01
Total	100.28	100.11	100.06	100.59	100.05	101.30	97.17	97.44	97.23	94.95	94.61
Atomic proportions											
Si	0.999	0.986	1.888	1.955	1.971	1.945	6.038	6.541	7.149	5.532	5.822
Ti	-	-	0.041	0.021	0.009	0.027	0.423	0.257	0.169	0.713	0.413
Al	0.002	0.002	0.143	0.060	0.039	0.039	2.114	1.437	0.865	2.429	1.845
Fe <sup>3+</sup>	-	-	0.057	0.063	0.428	0.871	-	0.250	0.175	-	-
Fe <sup>2+</sup>	0.933	1.833	0.239	0.674	0.448	0.034	3.192	4.068	4.126	1.789	5.383
Mn	0.019	0.083	0.004	0.014	0.032	0.018	0.051	0.097	0.181	0.008	0.171
Mg	1.038	0.093	0.679	0.232	0.065	0.020	1.170	0.349	0.337	3.115	0.235
Ca	0.008	0.021	0.890	0.910	0.581	0.182	1.860	1.523	0.848	-	0.017
Na	-	-	0.057	0.063	0.428	0.871	0.816	1.229	1.910	0.061	0.146
K	-	-	-	-	-	-	0.328	0.343	0.344	1.854	1.773
F	-	-	-	-	-	-	0.121	0.098	0.375	0.161	0.007
O	4.000	4.000	6.000	6.000	6.000	6.000	23.000	23.000	23.000	22.000	22.000
End members (Fe = Fe <sup>2+</sup> in analyses 1 to 6, = $\frac{1}{2}$ Fe in analyses 7 to 11)											
Mg	52.17	4.63	69.35	23.60	6.68	2.17	21.05	5.51	4.76	63.42	4.06
Fe+Mn	47.83	95.37	24.86	70.01	49.33	5.53	58.68	69.68	63.37	36.58	95.94
Na+K	-	-	5.78	6.39	43.99	92.30	20.59	24.81	31.87	-	-

\*Fe<sub>2</sub>O<sub>3</sub>, where shown, is calculated by theoretical cation balance (see text); FeO by difference.

Sample numbers below refer to the Geological Survey of Greenland collection, except for analysis 10.

1. olivine	86120	chilled gabbro	5. pyroxene	186233	foyaite	9. amphibole	186233	foyaite
2. olivine	86127	augite-syenite	6. pyroxene	186233	foyaite	10. biotite	ARM/116/80	chilled gabbro
3. pyroxene	86120	chilled gabbro	7. amphibole	86041	syenogabbro	11. biotite	186233	foyaite
4. pyroxene	86100	augite-syenite	8. amphibole	86127	augite-syenite			

alkali feldspar rims exhibit fine, micropertthitic intergrowths, but outer zones commonly appear homogeneous. Subidiomorphic, tabular alkali feldspar is typically the only feldspar present in the augite-syenites. It is usually cryptoperthitic but sometimes exhibits combined albite/pericline twinning in the plagioclase component. Almost all feldspars in the foyaites are coarsely perthitic.

Twenty-three probe analyses of feldspars from the border-group are plotted together with four chemical analyses from Upton (1964a) in fig. 7. No attempt was made to obtain probe analyses from the coarsely exsolved feldspars of the central intrusion. However, seven bulk chemical analyses of separated feldspars from this part of the intrusion from Upton (1964b) are plotted.

The border-group feldspars define a single trend of continuous solid-solution. The most calcic plagioclase cores, which occur in the chilled margins, are only just in the labradorite range (An<sub>53</sub>). Zoning is restricted in most crystals from the chilled margin but one rim of An<sub>21</sub>Ab<sub>79</sub>Or<sub>9</sub> was detected. Feldspars from the syenogabbros are intensely zoned within the range labradorite An<sub>52</sub>-anorthoclase An<sub>15</sub>Ab<sub>70</sub>Or<sub>15</sub>-sanidine' An<sub>4</sub>Ab<sub>54</sub>Or<sub>42</sub> and approach the plagioclase-alkali feldspar cotectic. Bulk-analyses of feldspars from the central group define a separate group of Ca-free alkali feldspars which were probably soda-sanidines prior to unmixing. Within this group, the feldspar compositions become more K-rich eastwards in the dyke, in contrast to the increasingly sodic nature

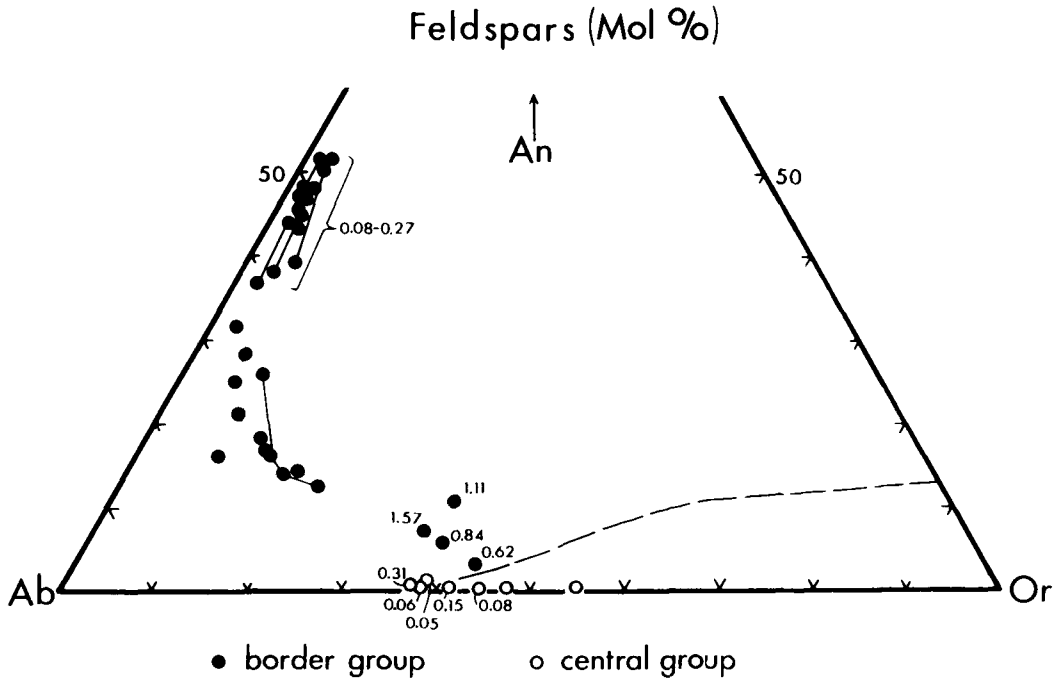


FIG. 7. Feldspar analyses from the OGDC projected into Ab–An–Or. Probe-analyses (this study) and analytical data from Upton (1964*a* and *b*). Solid circles: border group (probe and bulk analyses). Open circles: central group (bulk analyses only). The position of the 5 kbar cotectic (dashed line) is for comparative purposes only. Values of BaO (oxide wt. %) are indicated where available. Tie lines denote zonal range in individual crystals.

of the whole-rock compositions. This continuing trend of K-enrichment in alkali feldspars, beyond the projected position of the experimental 5 kbar cotectic, is a feature of other Gardar Si-undersaturated suites (Chambers, 1976; Stephenson, 1976; Jones, 1980). It suggests that the true position of the cotectic lies nearer to the Or corner in such suites, owing to the presence in the system of other components, notably nepheline, into which Na is preferentially incorporated. However, whereas in the South Qôroq Centre the feldspars form a smooth trend of continuous K-enrichment (Stephenson, 1976), in similar rocks from the OGDC there appear to be two separate feldspar trends, suggesting a petrogenetic discontinuity between crystallization of the border and central groups.

Ba values are low in the more-calcic plagioclases but increase to a maximum of 1.57 wt. % BaO (equivalent to 2.82 mol. % celsian) in anorthoclase rims from the more-fractionated syenogabbros. Values then fall rapidly with increasing  $K_2O$  in the soda-sanidines (fig. 7).

*Olivines* (48 analyses). Early crystallized olivine is a major constituent of the border-group mafic

rocks. In the central group the olivine decreases eastwards from the augite-syenites to the pulaskites and the degree of oxidation and replacement by iddingsite increases. In common with most other Gardar suites, olivine became unstable in the more alkaline residual magmas in which sodic pyroxenes crystallized (Stephenson and Upton, 1982) and olivine is consequently absent from the foyaites E. of the Central Complex.

The most magnesian olivines of the chilled margin are  $Fe_{53}$ , comparable with those of other Gardar alkali gabbros. Upton and Thomas (1980) related the relatively Fe-rich character of the early olivines to the late crystallization of magnetite in strongly reduced (dry) magmas. In the marginal syenogabbros compositions extend to  $Fe_{16}$ , zoning is slight and the range in individual rocks is less than 5% Fo. The overall trend (fig. 8) shows a compositional gap between  $Fe_{39}$  and  $Fe_{23}$  comparable to that of the oversaturated Klokken Complex (Parsons, 1979). However, whereas at Klokken the gap occurs between two intrusive units, in the OGDC the gap occurs within the marginal group. Parsons (1979) suggested that the gap may have resulted from a sudden drop in

temperature and an increase in water content of the magma. This suggestion is supported in the OGDC by the sudden appearance of intercumulus amphibole in syenogabbros having olivines in the range  $FO_{23-16}$ .

The slight gap between compositions obtained from the marginal group and central group ( $FO_{16-10}$ ) is not considered significant and compositions in the augite-syenites and pulaskites span a short range ( $FO_{10-4}$ ). Relatively high values of Mn and Ca throughout are comparable with those of olivines from most other Gardar suites. The forster-

ite-fayalite-tephroite trend (fig. 8) is colinear with those of all Gardar suites except for those of the unusually Mn-enriched Igaliko Complex (Stephenson, 1974; Chambers, 1976; Powell, 1978; Jones, 1984).

*Clinopyroxenes* (117 analyses). Clinopyroxene is a major constituent of most rocks of the dyke complex. In the syenogabbros, and in the augite-syenites west of the fjord crossing the western part of the intrusion, the pyroxene is a pinkish brown, slightly zoned salite. In the augite-syenites east of the fjord, green rims of sodic pyroxene appear and

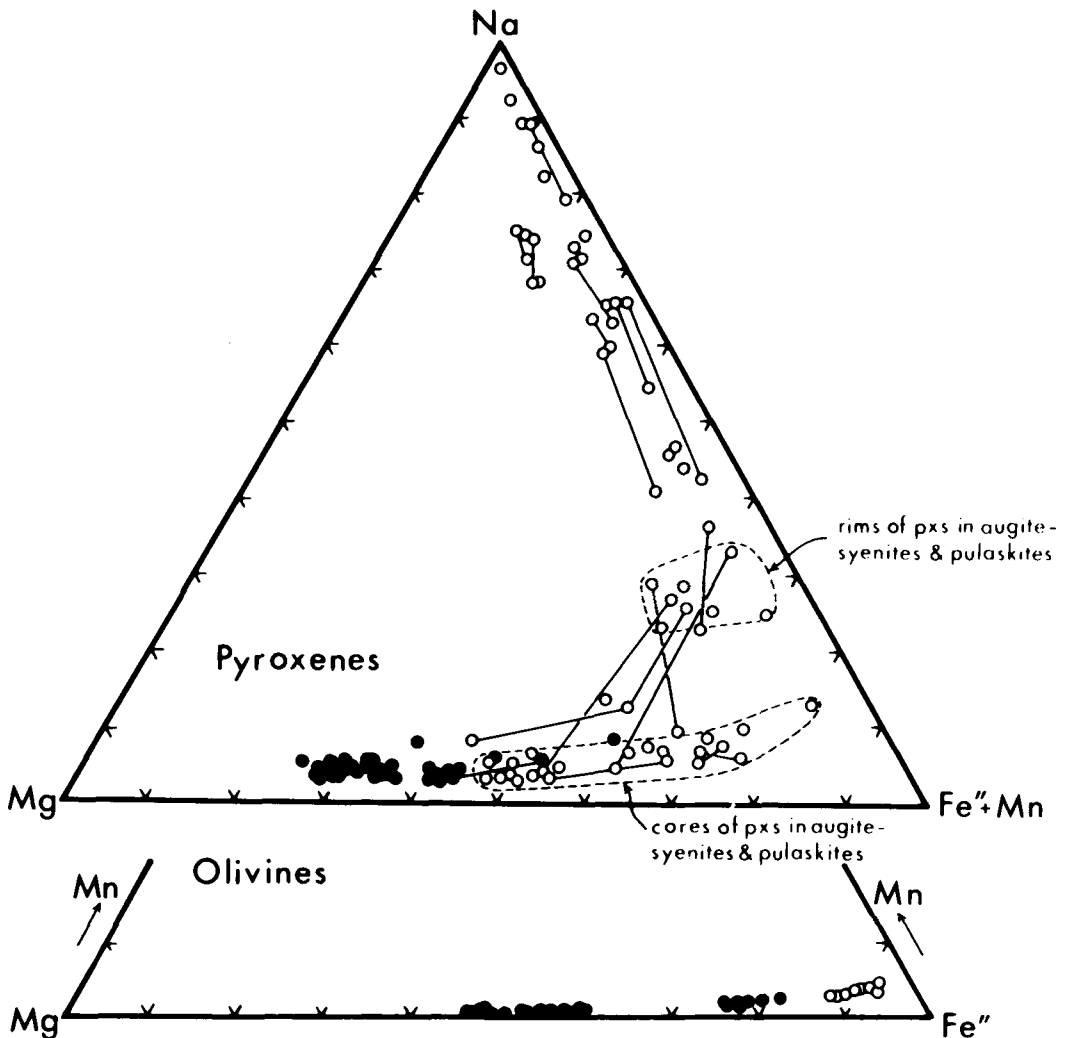


FIG. 8. Olivine and clinopyroxene compositions from the OGDC. Tie-lines are shown, where possible, to illustrate the range within individual clinopyroxene crystals. (Na) is total Na and therefore includes a small amount of the jadeite molecule in addition to acmite. Symbols as for fig. 7.

in the pulaskites, pleochroic, green aegirine-augite is dominant. In the foyaites, the clinopyroxene cores crystallized early but interstitial growth has produced strongly-zoned, deep green aegirine-augites. At the eastern end of the dyke all the pyroxene is interstitial to the alkali feldspar and nepheline and outer zones consist of almost pure, pale-green aegirine.

The overall compositional trend (fig. 8) is comparable to those obtained from the Si-under-saturated Igaliko Centres (Stephenson, 1972; Chambers, 1976; Powell, 1978; Jones, 1984), with a continuous variation from  $Di_{69}Hd_{27}Ac_4$  to  $Di_2Hd_2Ac_{96}$ . Na-enrichment occurs at a relatively early stage, suggesting the presence of peralkaline interstitial liquids during the later stages of pyroxene growth in some augite-syenites and in all the more-evolved rocks. Zoning is pronounced in all the sodic pyroxenes. The trend shows no compositional breaks such as that observed in the olivines and zoning causes considerable overlap of pyroxene compositions between samples. Of particular note is the overlap between pyroxene rims from the more evolved syenogabbros and pyroxene cores from the central-group augite-syenites. Pyroxene core compositions form a progressive sequence from the chill to the inner edge of the border-group, and from W. to E. along the dyke centre and hence they are indicative of the state of magma evolution represented by each rock.

Minor element variation is comparable with that in pyroxene series from other Gardar under-

saturated suites (Stephenson, 1972; Chambers, 1976; Larsen, 1976; Powell, 1978; Jones, 1984). Values of Al and Ti in pyroxenes fall suddenly within the syenogabbro compositions, coincident with the gap in olivine compositions (cf. Parsons, 1979). Al values then fall more gradually and level-out at around 0.04 atoms per 6 oxygens in the aegirine-augites and aegirines due to the presence of  $Al^{VI}$  in small amounts of the jadeite molecule.

*Amphiboles* (51 analyses). Amphibole appears as a late, minor phase in the more-evolved syenogabbros at the inner edge of the border-group. In the central-group, amphibole is relatively abundant throughout the augite-syenites and pulaskites as pleochroic muddy-brown rims on pyroxenes. In the more evolved rocks the amphibole zones outwards to a blue-green variety and occupies interstitial areas. Blue-green amphibole is abundant in some foyaites, but decreases eastwards and is scarce or absent from aegirine-bearing rocks east of the cross-cutting YGDC. Analyses were recalculated to a total of 13 cations (excluding Ca, Na, and K) in order to partition  $Fe^{II}$  and  $Fe^{III}$  and were classified according to the IMA scheme (Leake, 1978) using a computer program (Rock and Leake, 1984). Expressed simply in terms of  $(Al^{IV})_T$  and  $(Na)_B$  the analyses fall mostly within a range from ferropargasite or hastingsite (depending on the  $Al^{VI}/Fe^{III}$  ratio) to katophorite, with slight extension towards arfvedsonite in the more-evolved compositions (fig. 9). The overall trend is thus comparable with amphibole trends from other Gardar

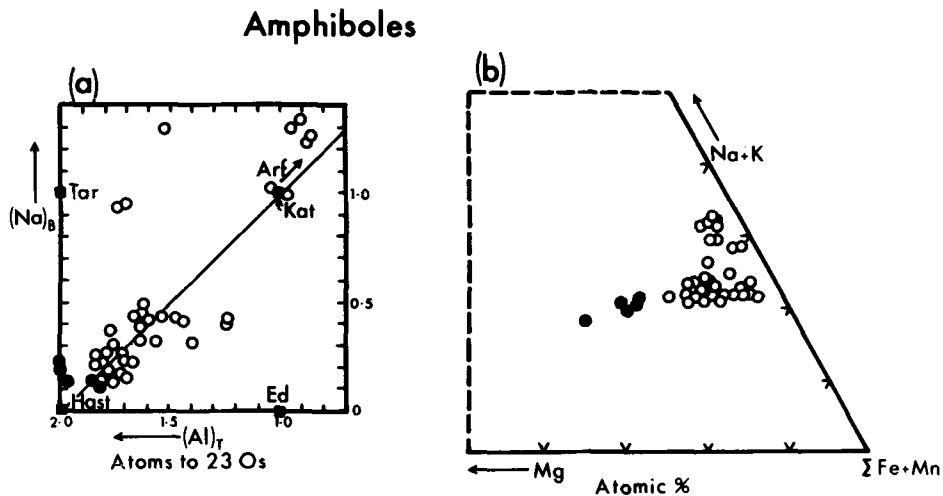


FIG. 9. Amphibole compositions for the OGDC. Symbols as for fig. 7. (a) Classification parameters  $(Na)_B$  v.  $(Al^{IV})_T$ . The 1:1 line represents ideal substitution of the form  $(Na)_B + (Si)_T = (Ca)_B + (Al)_T$ . End members: Arf, arfvedsonite; Ed, edenite; Hast, hastingsite (or pargasite); Kat, Katophorite; Tar, taramite. (b)  $(Na + K)$  v. Mg v.  $(Fe + Mn)$  for comparison with the clinopyroxene trend.

Si-undersaturated suites (Stephenson and Upton, 1982). In detail, high Al contents, such that  $Al^{VI} > Fe'''$ , commonly result in a pargasitic classification and all of the more-primitive compositions qualify for titanian and potassian prefixes. Amphiboles from each rock type may be summarized as:

Syenogabbro: titanian, potassian (ferroan pargasite-ferro-pargasite-hastingsite).

Augite-syenite: titanian, potassian (ferro-pargasite-ferro-pargasitic hornblende-hastingsitic hornblende).

Pulaskite: hastingsitic hornblende.

Foyaite: potassian katophorite (with potassium tarimate in one sample).

Changes in Mg/Fe are dominant in the syenogabbros and augite-syenites [ $(Mg)_C \rightarrow (Fe'')_C$ ], but in the pulaskites and foyaites alkali-enrichment is dominant [ $(Ca)_B + (Mg, Fe'')_C \rightarrow (Na)_B + (Fe''')_C$ ], accompanied by a general decrease in  $Al^{IV}/Si$  [ $(Ca)_B + (Al)_T \rightarrow (Na)_B + (Si)_T$ ]. Amphibole compositions become more-evolved from W. to E. along the dyke and also correlate well with the rim compositions of enclosed pyroxenes, so emphasizing the reaction relationship.

**Biotites** (66 analyses). Biotite occurs in all the basic rocks of the border-group as reaction fringes on Fe-Ti oxides. It is particularly abundant in the augite-syenites at the SW end of the OGDC, both as reaction rims and in interstitial areas, but decreases in abundance eastwards. In the foyaites it occurs rarely, in association with amphibole, and is absent from the most-evolved rocks.

Analyses were recalculated to 22 oxygens on a water-free basis and are shown in fig. 10. As in other Gardar suites, the variation is almost entirely in terms of changing Fe/Mg, with a wide range from annite<sub>32</sub> to annite<sub>100</sub>. It is likely that most of the biotites contain a significant amount of  $Fe'''$  and are therefore lepidomelanes. Zoning, where present, is commonly reversed, possibly reflecting inward growth from the margins of interstices. The trend is continuous, with marked variation between individual rocks, especially in the more basic rocks and augite-syenites. The biotites therefore provide a useful evolutionary index for the interstitial liquids of these rocks. Mn shows a gradual increase with Fe/Mg, with a wide scatter in the most evolved compositions. This may reflect a trend, comparable to that of the earlier-crystallizing olivines, in which Mn-enrichment became dominant in the later stages of evolution, after Fe/Mg had reached a maximum. The most-evolved composition, from a foyaite, is phlogopite<sub>3</sub>annite<sub>94</sub>manganophyllite<sub>3</sub>, which is richer in Mn than any in the oversaturated Klokken and Kungnät Complexes, but not as rich as in the undersaturated Igaliko Centres (cf. a similar comparison in the olivines).

Ti is generally high but reduces slightly in

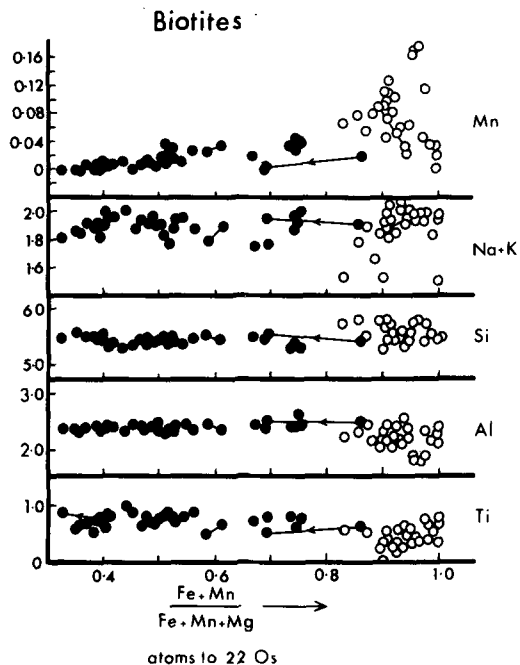


FIG. 10. Biotite compositions for the OGDC. Symbols as for fig. 7. A few tie-lines are shown on which arrows point from core to rim. The apparent reversed zoning is a function of inward interstitial growth.

more-evolved compositions. Other elements show only slight, non-systematic variation with no gaps or sudden 'jumps' in value such as are observed in the Kungnät Complex. (Si + Al) is very close to the stoichiometric ideal of 8 throughout the series.

**Iron-titanium oxides** (55 magnetite, 26 ilmenite analyses). Titaniferous magnetite is an important early-crystallizing phase in the syenogabbros and augite-syenites, but decreases in abundance eastwards along the central-group. Discrete tabular crystals of ilmenite are confined to the border-group where they are more numerous close to the chilled margins. Even here they often exhibit very fine exsolution trellises, possibly of hematite. Most rocks of the border-group and some of the more basic augite-syenites of the central-group contain magnetite and ilmenite as rounded grains ('clustered granules') which may be a result of an early exsolution event (cf. Parsons, 1979). In most of the augite-syenite samples, magnetite contains trellises of broad ilmenite lamellae, due to low-temperature exsolution and oxidation, but these are less well developed in the more evolved rocks. Secondary magnetite occurs as reaction rims on the more evolved olivines, and may also be derived from aegirine-augite in some foyaites.

Table II. Representative analyses of iron-titanium oxides from the Tugtutôq Older Giant Dyke Complex.

	1	2	3	4	5	6	7
SiO <sub>2</sub>	0.34	0.21	0.25	0.23	0.30	-	0.24
TiO <sub>2</sub>	21.01	51.77	19.86	50.35	4.59	1.00	52.17
Al <sub>2</sub> O <sub>3</sub>	3.04	-	0.41	-	-	0.05	-
Fe <sub>2</sub> O <sub>3</sub> *	21.92	1.65	29.38	2.67	59.46	64.46	0.71
FeO	50.15	43.94	48.28	43.68	33.31	30.88	45.93
MnO	0.47	0.58	1.27	1.85	2.11	0.01	0.88
MgO	-	1.28	-	-	-	-	0.22
ZnO	0.34	-	0.30	-	0.34	-	-
Total	97.26	99.43	99.75	98.78	100.10	96.41	100.15
Atomic proportions							
Si	0.112	0.011	0.084	0.012	0.116	-	0.013
Ti	5.226	1.969	5.036	1.954	1.343	0.320	1.979
Al	1.186	-	0.164	-	-	0.026	-
Fe <sup>3</sup>	5.463	0.063	7.463	0.104	17.443	20.446	0.027
Fe <sup>2</sup>	13.870	1.858	13.615	1.885	10.846	10.871	1.937
Mn	0.131	0.025	0.364	0.081	0.695	0.005	0.038
Mg	-	0.097	-	-	-	-	0.017
Zn	0.083	-	0.074	-	0.099	-	-
O	32.000	6.000	32.000	6.000	32.000	32.000	6.000
End members							
% Usp	61.42	-	57.31	-	14.32	3.03	-
% R <sub>2</sub> O <sub>3</sub>	-	4.00	-	2.62	-	-	0.72

\* Fe<sub>2</sub>O<sub>3</sub> is calculated by theoretical cation balance (see text)

Sample numbers below refer to Geological Survey of Greenland collection.

1. magnetite 86120 chilled gabbro
2. ilmenite 86120 chilled gabbro
3. magnetite 86100 augite-syenite
4. ilmenite 86100 augite-syenite
5. magnetite 86036 foyaite
6. magnetite 40487 foyaite - secondary
7. ilmenite 86126 syenogabbro-lamellae

Separate analyses were made of magnetite and ilmenite phases in each rock (Table II). No attempt was made to obtain bulk analyses of exsolved grains. The analyses were recalculated to determine Fe<sup>III</sup>/Fe<sup>II</sup> assuming that they were members of magnetite-ulvöspinel and ilmenite-hematite solid solutions (fig. 11). Minor oxides were allocated to end-members according to the method of Carmichael (1967). The mafic border group rocks and augite-syenites exhibit little order in magnetite compositions, except that zoning, which can be up to 43% Usp., is usually in the direction of Ti-enrichment. Rocks in which magnetite and ilmenite occur as separate grains have magnetite in the range Usp<sub>4.4-6.7</sub> and ilmenite in the range Hem<sub>0.6-4.0</sub>. Rims of strongly zoned magnetite and magnetite with exsolved ilmenite are in the range Usp<sub>68-86</sub>. Exsolved ilmenite lamellae are always

nearly pure (Hem<sub>0-0.5</sub>). The trend towards Ti-enrichment is reversed in the pulaskites and foyaites, in which magnetites are generally less titaniferous within the range Usp<sub>28-13</sub>, with lamellae poorly developed or absent. Altered foyaite contains almost pure magnetite (Usp<sub>2-6</sub>) which is probably derived from the oxidation and break-down of aegirine-augite.

In view of the uncertainty which now exists concerning the validity of different methods of calibrating the Fe-Ti oxide geothermometer and oxygen barometer (Buddington and Lindsley, 1964; Powell and Powell, 1977; Spencer and Lindsley, 1981), numerical estimates of crystallization conditions obtained by this method must be treated with extreme caution. Differences of up to 150 °C and 4 log units of *f*<sub>O<sub>2</sub></sub> are common between results from the various methods and further variation

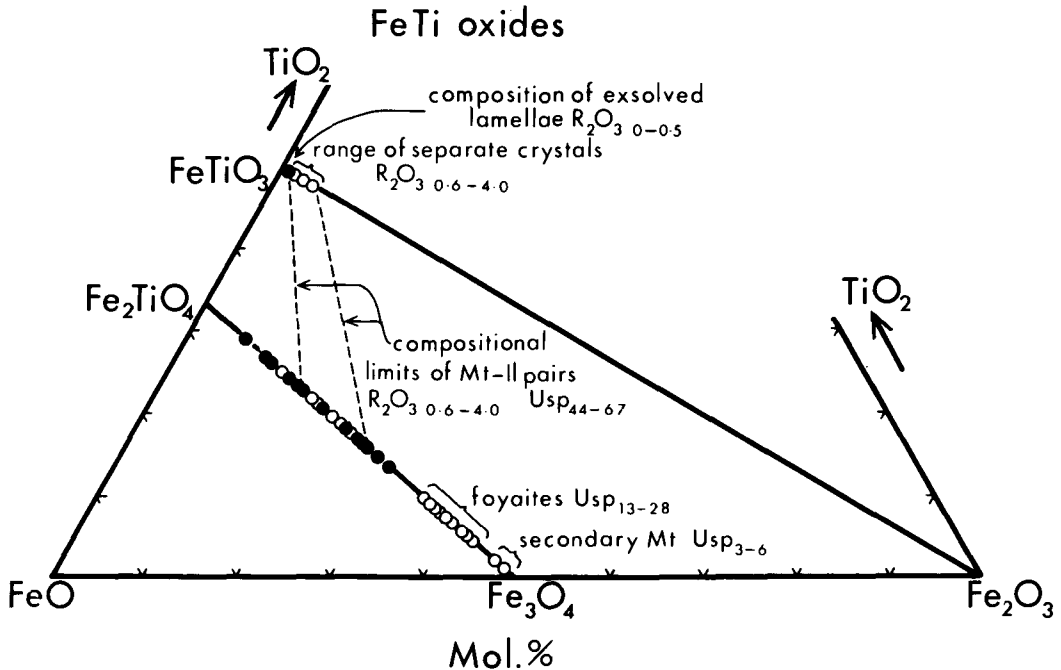


FIG. 11. Fe-Ti oxide compositions for the OGDC. Analyses are recalculated to theoretical magnetite (Mt)-ulvöspinel (Usp) and ilmenite (Ilm)-hematite (Hem) solid-solutions in order to allocate  $\text{Fe}^{3+}$  and  $\text{Fe}^{2+}$ .  $\text{R}_2\text{O}_3$  = hematite + all other trivalent cation oxides. Symbols as for fig. 7. Analyses of separate coexisting grains of titanomagnetite and ilmenite fall in the restricted field shown. Some of the scatter in the other titanomagnetite analyses may be due in part to varying degrees of ilmenite exsolution. Many analyses have been omitted for clarity.

may be introduced according to the method of allocating minor oxide components to end-members (Stormer, 1983). Two samples from the OGDC chilled margin yield values of  $844^\circ\text{C}/-14.4 \log_{10} f_{\text{O}_2}$  and  $747^\circ\text{C}/-16.8 \log_{10} f_{\text{O}_2}$  by the Buddington and Lindsley calibration (calculated by the method of Powell and Powell, 1977) and  $750^\circ\text{C}/-17.2 \log_{10} f_{\text{O}_2}$  and  $635^\circ\text{C}/-20.5 \log_{10} f_{\text{O}_2}$  by the Spencer and Lindsley calibration. In each case the values are the highest possible  $T$  and  $f_{\text{O}_2}$  obtainable from the analyses (i.e. maximum observed % Usp in magnetite and maximum observed % Hem in ilmenite). Both samples lie just below the synthetic QFM buffer curve on both calibrations (variation between calibrations usually results in a displacement parallel to the synthetic buffer curves).

**Apatites.** Apatite appears to have been in equilibrium with the already P-rich initial magmas represented by the chilled marginal samples. Euhedral apatite is abundant (several modal %) in the border group rocks and diminishes in amount and crystal-size from the augite-syenites to the foyaites.

A separate study of apatites from differentiated Gardar rock suites (P. Hill, pers. comm.) has covered those of the OGDC. The CaO content of the apatites falls with increasing differentiation reflecting falling whole-rock values. Cl is clearly strongly fractionated into early apatites and falls sharply to below detection limits in the syenite apatites. By contrast F remains constant at  $c.3\%$  throughout the OGDC apatites, i.e. the F/Cl ratio rises with fractionation. The OGDC apatites are notably richer in F and marginally poorer in Cl for any specific CaO value than those from the YGDC. It is of interest that the F and Cl contents of the chilled margins (whole-rock) are much higher in the OGDC than in the YGDC (F = 1980 ppm, cf. 620 ppm: Cl = 190 ppm cf. 60 ppm: Upton and Thomas, 1980), although the F/Cl ratios (10.4 and 10.3) are nearly identical.

#### Whole-rock chemistry

Representative analyses of OGDC samples are presented in Table III. The initial magma, as indicated by chilled (aphyric) marginal facies was a

# THE TUGTUTÔQ OLDER GIANT DYKE COMPLEX

635

Table III. Representative analyses of rocks from the Older Giant Dyke Complex

Major elements (Wt%)								
	1	2	3	4	5	6	7	8
SiO <sub>2</sub>	42.76	41.91	44.73	57.59	58.26	57.93	54.52	55.26
Al <sub>2</sub> O <sub>3</sub>	15.57	13.06	13.41	16.67	16.43	16.54	18.85	18.87
FeO*	14.31	17.88	16.30	7.43	7.50	8.45	6.88	6.97
MgO	5.02	4.11	3.32	0.72	0.64	0.31	0.17	0.20
CaO	8.52	8.08	7.62	2.78	2.79	2.39	1.44	0.74
Na <sub>2</sub> O	3.05	3.31	3.96	6.32	5.95	6.21	9.67	7.82
K <sub>2</sub> O	1.48	1.74	2.34	5.47	5.55	5.94	5.39	5.08
TiO <sub>2</sub>	4.41	4.53	3.35	1.01	0.95	0.54	0.30	0.31
MnO	0.19	0.26	0.27	0.16	0.18	0.20	0.17	0.17
P <sub>2</sub> O <sub>5</sub>	2.28	3.08	2.67	0.24	0.25	0.10	0.04	0.04
L.O.I	0.23	0.50	-	0.65	0.69	-	1.88	3.53
Totals	97.82	98.46	97.97	99.04	99.19	98.61	99.31	98.99
Trace-elements. (p.p.m.)								
Ni	26	5	6	2	2	4	3	2
Cr	7	7	24	4	5	4	6	5
V	168	95	46	5	3	2	-	-
Sc	14	16	21	12	12	1	-	-
Cu	40	127	36	7	13	21	3	-
Zn	72	106	103	101	190	99	170	225
Sr	1186	939	863	255	217	89	21	25
Ba	1477	1821	2779	2105	1722	118	35	29
Rb	27	33	34	96	154	161	241	222
Pb	-	-	-	13	29	16	33	45
Th	-	-	-	4	16	12	23	36
Zr	136	176	199	518	678	614	897	1783
Nb	25	39	43	74	113	91	143	285
Y	33	50	57	49	89	47	61	157
La	39.3	65.0	75.2	68.9	94.4	106.4	119.5	252.8
Ce	89.3	148.2	169.6	148.0	203.5	233.8	252.3	540.8
Pr	12.8	19.2	22.5	16.5	22.6	25.9	25.0	56.6
Nd	51.9	81.6	92.8	60.6	85.6	96.4	88.2	206.7
Sm	9.4	14.7	16.3	10.5	16.6	16.0	14.1	35.4
Eu	3.5	4.6	5.1	3.2	3.4	1.7	1.1	2.9
Gd	9.1	13.8	14.8	13.5	18.7	15.7	19.5	35.9
Dy	5.8	8.9	10.1	8.2	15.2	9.5	9.1	24.2
Ho	1.1	1.7	2.0	2.0	3.3	2.1	2.5	5.3
Er	2.7	4.2	5.2	4.8	8.3	5.7	5.1	12.5
Yb	2.2	3.4	3.8	4.5	7.4	5.9	4.6	8.3
Lu	0.3	0.5	0.6	0.7	1.1	1.1	0.8	1.1
C.I.P.W. Norms								
or	8.96	10.44	14.04	32.82	33.26	35.50	32.47	33.48
ab	23.39	28.48	29.92	39.51	41.74	38.45	20.85	17.65
an	24.90	15.89	12.10	0.94	1.74	-	-	-
ne	-	-	2.26	8.00	5.04	7.64	25.70	25.90
ac	-	-	-	-	-	0.52	13.39	17.12
di	2.52	3.75	7.35	9.95	9.25	9.97	3.57	3.78
hy	3.57	1.68	-	-	-	-	-	-
wo	-	-	-	-	-	-	1.20	-
ol	16.36	19.59	17.78	4.01	4.30	2.44	-	0.69
mt	3.22	4.01	3.66	2.23	2.25	4.23	2.13	0.66
tl	8.56	8.75	6.48	1.95	1.84	1.03	0.59	0.64
ap	5.52	7.41	6.43	0.57	0.60	0.23	0.09	0.09
D.I.	35.35	38.93	46.21	80.33	80.03	81.58	79.03	77.03

- |                                 |                         |
|---------------------------------|-------------------------|
| 1. 86120 Olivine gabbro (chill) | 5. 86108 Augite syenite |
| 2. 30684 Syenogabbro            | 6. 30640 Pulaskite      |
| 3. 40430 Syenogabbro            | 7. 86035 Foyaite        |
| 4. 86116 Augite syenite         | 8. 85999 Foyaite        |

C.I.P.W. norms: Appropriate Fe<sub>2</sub>O<sub>3</sub>/100/(FeO + Fe<sub>2</sub>O<sub>3</sub>) values selected on the basis of FeO and Fe<sub>2</sub>O<sub>3</sub> determinations presented in Upton (1964b). Analyses 1, 2 and 3, 15%; Analyses 4 and 5, 20%; Analysis 6, 35%; Analyses 7 and 8, 80%.

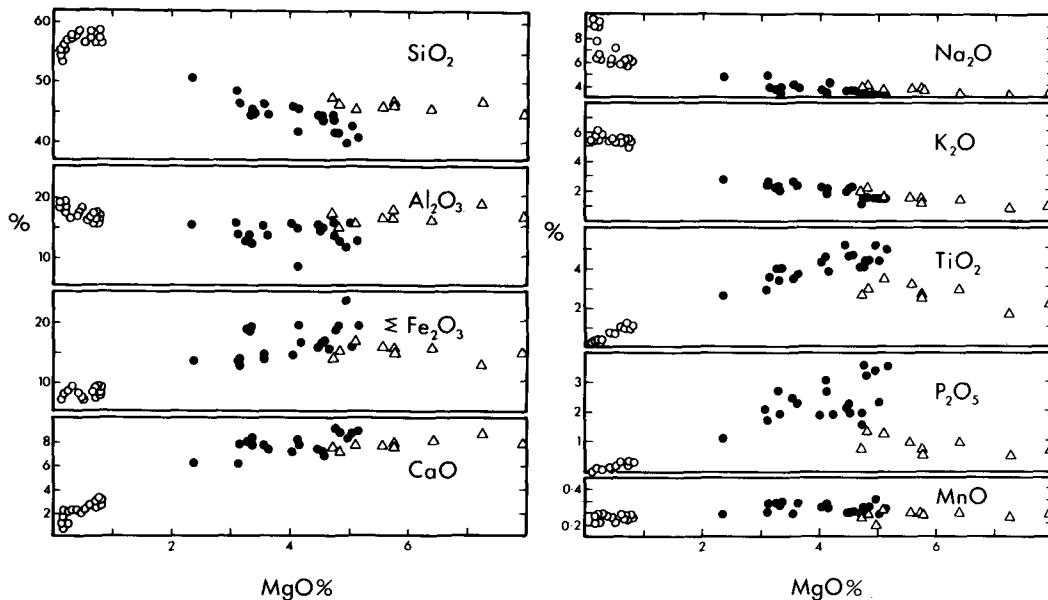


FIG. 12. Major elements in OGDC whole-rock samples *v.* MgO wt. %. Border-group samples, closed circles; central group, open circles. Open triangles indicate compositions of chilled marginal facies rocks from the younger giant dyke complex.

relatively Fe-rich alkali olivine basalt verging to hawaiite (Table III, col. 1). From the petrography it appears that olivine, plagioclase, ilmenite, Ti magnetite, and apatite (but not augite) were all in equilibrium with the liquid at the time of emplacement. Augite, as in the YGDC (Upton and Thomas, 1980), appears to have commenced crystallization at a relatively late stage in the cooling history.

On petrographic grounds, it is concluded that the oxidation state of the OGDC magmas increased with progressive differentiation. Observed  $\text{Fe}_2\text{O}_3 \cdot 100/(\text{FeO} + \text{Fe}_2\text{O}_3)$  values increase from  $< 20$  to  $> 80$ , from gabbros to foyaites; accordingly the values (15–80%) used in Table III for the calculation of the norm are those thought to be most appropriate for the various compositions.

Variation diagrams for major and trace elements *v.* MgO% are shown in figs. 12 and 13. Although only 3 of the 40 analysed samples can (as chilled marginal samples) be regarded as close to liquid compositions, the trends displayed may give a reasonable semblance to the line of liquid descent. Samples collected in a traverse perpendicular to the (N) chilled margin in the fjord section towards the west end of the intrusion show that the border-group exhibits a generalized trend towards increasingly fractionated compositions from the contact wall inwards:  $\text{SiO}_2$ ,  $\text{Na}_2\text{O}$ , and  $\text{K}_2\text{O}$  rise whereas  $\text{Fe}_2\text{O}_3$ , MgO, CaO,  $\text{TiO}_2$ , and  $\text{P}_2\text{O}_5$  decrease.

$\text{Al}_2\text{O}_3$  and MnO remain relatively constant and the Mg-number serially diminishes (fig. 14). Among the trace-elements in the border-group, Ba increases notably while Sr falls steadily; Ni, Cu, and V show an overall decrease, Sc remains roughly constant and Rb, Zr, Nb, Y, and REE increase.

Although there is a very marked compositional hiatus, the variation trends of the central-group can be construed as lower-temperature continuations of those of the border-group. However, the increase in  $\text{SiO}_2$  with rising Fe/Mg in the border-group gives way to a decline in the central-group as alkalis and alumina increase sharply. Ba increases from c.1400 ppm to c.4500 ppm in the border-group while, with increasing fractionation in the central-group, it falls from over 4000 to below 100 ppm in the more extreme foyaites. The behaviour of Ba suggests that in the 'missing compositions' represented by the hiatus (corresponding to a 'silica-gap' from 51 to 53%  $\text{SiO}_2$ ) Ba values well over 5000 ppm may be expected. The behaviour of Ba is reflected in the celsian contents of the feldspars, as noted above. By contrast Sr shows a shallow decline in the border-group followed by a steep decline in the central-group; there is thus no suggestion of a comparable Sr-peak.

It is the chondrite-normalized REE patterns (fig. 15) that bring out another striking difference between the border-group and the central-group

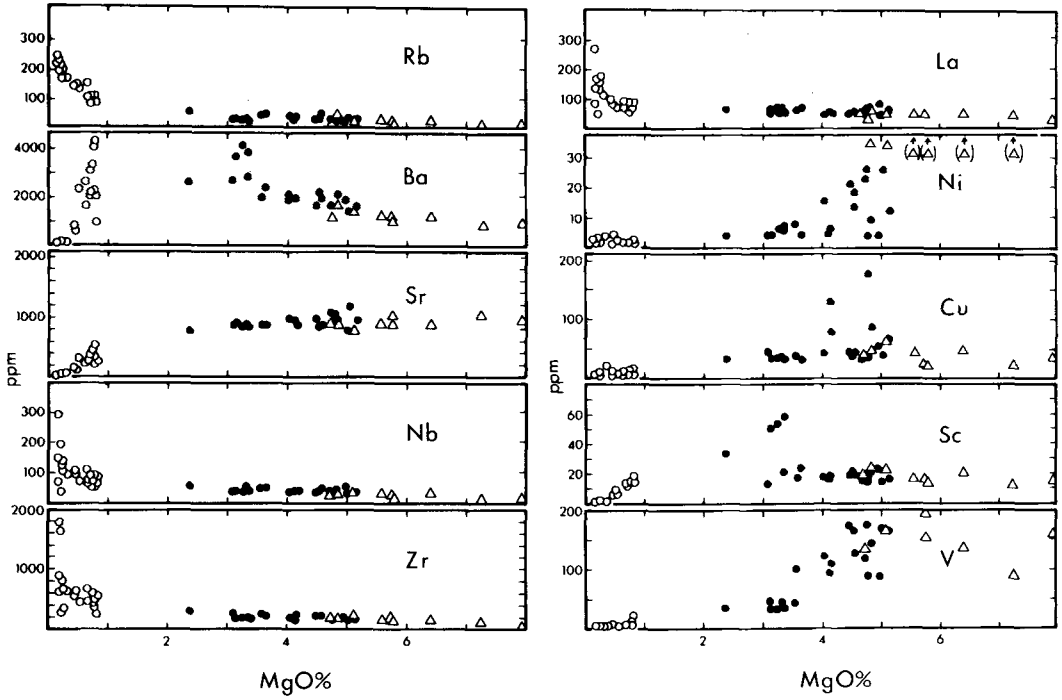


FIG. 13. Trace elements in OGDC whole-rock samples v. MgO wt. %.

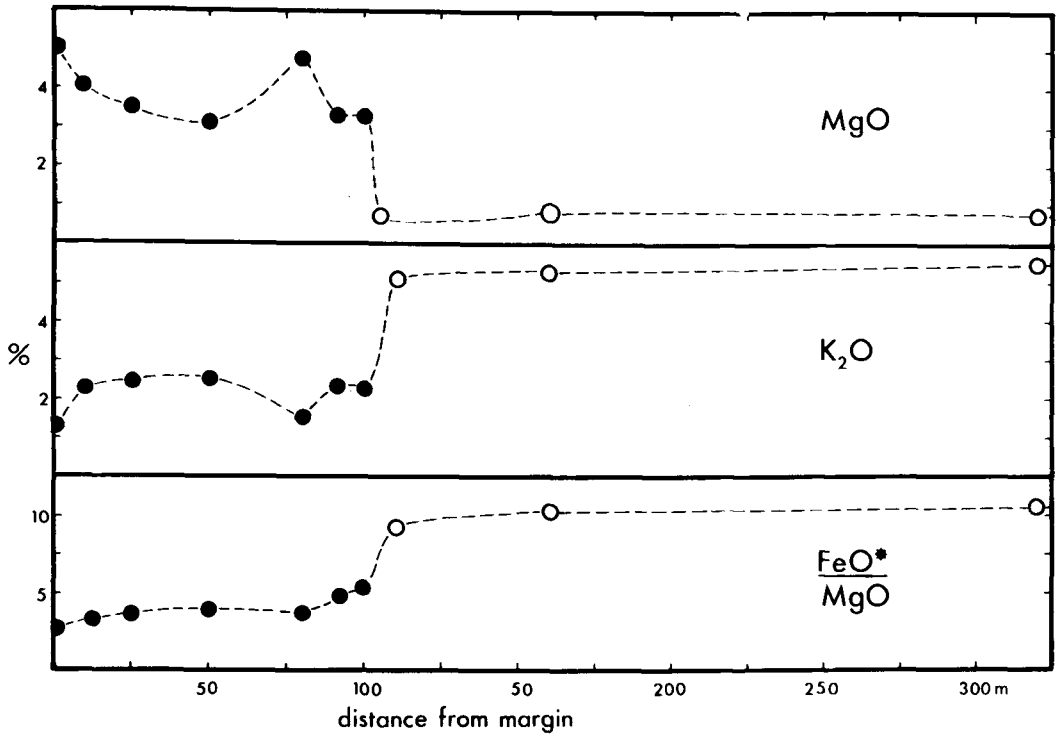


FIG. 14. Variation of MgO, K<sub>2</sub>O and FeO\*/MgO in OGDC samples with distance from contact. (Traverse from northern contact on W. coast of the fjord section across the western part of the intrusion.)

rocks. The border-group rocks show little or no indication of an Eu anomaly whereas the central-group rocks all possess a notable negative Eu anomaly. This anomaly is least marked in the augite-syenite sample and most marked in the foyaites.

In the border-group it is inferred that Eu and Sr were entering the plagioclase structure but that these were not being lost to the system, e.g. by gravitational removal of plagioclase crystals. However, the central-group negative Eu-anomalies imply that by the time the augite-syenites commenced crystallization a marked depletion in Eu (and Sr and Ca) had taken place. The inference is that the compositional hiatus between the two groups corresponds to the generation of an (unseen) suite of cumulates rich in plagioclase (i.e. a suite of relatively highly fractionated troctolitic or anorthositic cumulates). The plagioclase composition of these would have been more sodic than  $An_{53}$ . The anorthosite cumulate xenoliths of the

YGDC have feldspar compositions of  $An_{58-52}$ , i.e. rather more calcic than in the hypothesized cumulates required for the OGDC genesis.

However, the OGDC initial magma, like that of the YGDC, had no Eu anomaly. This, combined with its high Sr content (c.1200 ppm), suggests that it had, at the time of emplacement, undergone no significant plagioclase fractionation and cannot itself be regarded as having produced the inferred deep-seated anorthosite cumulates.

#### *Age and initial $^{87}Sr/^{86}Sr$ ratios*

Sr-isotope compositions were studied (by A.R.M.) in eight samples from the OGDC, selected to cover the compositional range. The results are given in Table IV and, graphically, in fig. 16. The regression omits one sample (86 ARM 80) giving an age of  $1154 \pm 16$  Ma and an initial ratio of  $0.70326 \pm 0.00026$  (errors quoted to  $2\sigma$ ). The MSWD of 7.9 indicates that the points lie on an errorchron and

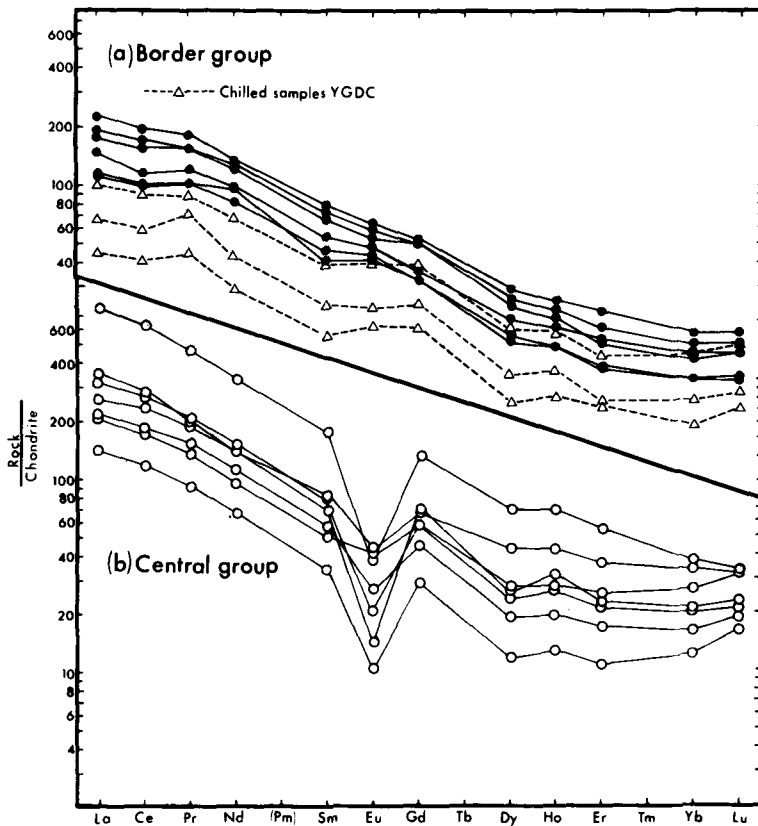


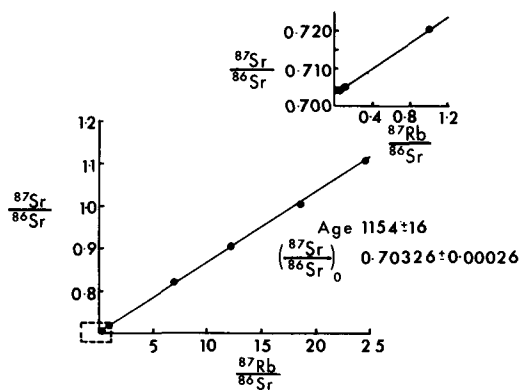
FIG. 15. Chondrite-normalized *REE* plots for (above), border-group mafic rocks and (below) central-group salic rocks. Open triangles denote data from YGDC chilled samples.

Table IV. Rb, Sr, Rb/Sr and  $^{87}\text{Sr}/^{86}\text{Sr}$  data for the O.G.D.C.

	Rb ppm	Sr ppm	Rb/Sr	$^{87}\text{Rb}/^{86}\text{Sr}$	$^{87}\text{Sr}/^{86}\text{Sr}$
86120	23.9	1096	0.022	0.0632 +/- 3	0.70411 +/- 3
40430	32.3	792	0.041	0.1180 +/- 6	0.70525 +/- 4
86/80	50.0	848	0.059	0.1708 +/- 9	0.70717 +/- 8
86116	93.0	254.3	0.366	1.059 +/- 3	0.72113 +/- 5
86014	164*	70*	2.34	6.93 +/- 3	0.81952 +/- 8
86036	258*	62*	4.16	12.13 +/- 6	0.90165 +/- 9
86013	199*	34*	5.85	18.50 +/- 9	1.0045 +/- 1
85999	207.1	25.4	8.154	24.6 +/- 1	1.1082 +/- 2

\* Determined by XRF

that there is some degree of inherent geological scatter. The data supersedes those of van Breemen and Upton (1972), which, using the decay constant then in use ( $1.39 \times 10^{-11}$  as opposed to  $1.42 \times 10^{-11}$  used here) gave an age of  $1150 \pm 9$  Ma and an initial  $^{87}\text{Sr}/^{86}\text{Sr}$  ratio of  $0.7024 \pm 0.0010$ . The revised initial ratio ( $0.70326 \pm 0.00026$ ) for the OGDC remains consistent with the hypothesis that the magmas derived from an alkali olivine basalt of mantle origin.

Fig. 16. Seven-sample  $^{87}\text{Sr}/^{86}\text{Sr}$  v. Rb/Sr errorchron for the OGDC.

### Giant dyke parent magmas

Fig. 17 shows chondrite-normalized incompatible element patterns for chilled margins of the OGDC and YGDC (means of 3 and 9 samples respectively). The patterns are similar with prominent Ba and P peaks and a trough at Nb. The OGDC pattern clearly reflects the higher content of incompatible elements and differs otherwise from that of the YGDC in showing a trough at Zr.

The OGDC chills, with higher  $\text{FeO}^*/\text{MgO}$ , incompatible element contents and lower compatible elements (e.g. Ni, Cr) appear distinctly more highly fractionated than those of the succeeding YGDC (Table V). However, the widely varying enrichment factors for incompatible elements in the OGDC, relative to those of the YGDC (e.g. Zr,  $\times 1.098$ ; P,  $\times 2.26$ ) appear to preclude any simple relationship by crystal fractionation and it is more likely that fundamental differences characterized the respective primary magmas. Considering also the REE patterns (fig. 15) in which the YGDC chills have less steep curves than those of the OGDC, it is inferred that the OGDC primary magma represented a smaller partial melt fraction than that parental to the YGDC. It is tentatively suggested that breakdown of apatite and phlogopite in the mantle source played a larger part in the genesis of the OGDC magmas and that higher K, Ba, Ti, P, LREE (and F) were features of the OGDC primary magma. It is proposed that the latter also possessed a higher alkali/silica ratio which firmly committed subsequent evolution to an undersaturated (foyaitic) trend. This contrasts with the more critical alkali/silica balance in the succeeding (and more voluminous) YGDC melting event where the ultimate residues, although mainly Si-oversaturated, also included some Si-undersaturated differentiates (Upton and Thomas, 1980).

### Discussion

As seen in the fjord section across the western part of the intrusion, there is some evidence that the border-group rocks become progressively more fractionated inwards from the chilled margins (fig. 11). At around 100 m in from the contacts the rocks change abruptly (within  $c.2$  m) from syenogabbroic with  $\text{MgO}$  values  $> 2.5\%$  and  $\text{SiO}_2 < 45\%$ , to syenitic ( $\text{MgO} < 1\%$ ;  $\text{SiO}_2 > 55\%$ ). However, despite this compositional hiatus, the tendency to

Table V. Mean analyses of chilled marginal samples  
from the OGDC and YGDC

	Major elements (wt%)	
	1	2
SiO <sub>2</sub>	43.47	46.00
Al <sub>2</sub> O <sub>3</sub>	15.65	16.71
FeO <sub>tot</sub>	14.02	13.43
MgO	4.76	5.93
CaO	7.70	7.78
Na <sub>2</sub> O	3.45	3.55
K <sub>2</sub> O	1.81	1.45
TiO <sub>2</sub>	4.40	2.63
MnO	0.19	0.19
P <sub>2</sub> O <sub>5</sub>	1.95	0.86
Totals	97.40	98.53
	Trace-elements (p.p.m.)	
Ni	22	52
Cr	5	30
V	138	160
Sc	16	17
Cu	40	39
Zn	81	90
Sr	1039	900
Ba	1669	1120
Rb	39	23
Pb	-	3
Zr	163	150
Nb	32	22
Y	35	27
La	47	27
Ce	104	64
Nd	57	34
K/Rb	385	504
Zr/Nb	5.1	6.8
La/Y	1.3	1.0
Ti/V	199	103
K <sub>2</sub> O/P <sub>2</sub> O <sub>5</sub>	0.92	1.68
FeO <sub>tot</sub> /MgO	2.95	2.26
Al <sub>2</sub> O <sub>3</sub> /CaO	2.03	2.15

1. Mean of 3 chilled marginal samples: OGDC.
2. Mean of 9 chilled marginal samples: YGDC.

become more fractionated towards the centre is still discernible in the augite-syenites (fig. 14). Thus, there is good reason to accept the original concept of a 2-pulse (composite) dilation (Upton, 1962) and to consider that both magmatic inputs tended to crystallize from the walls inwards. If so, the striking variation of syenite facies along the dyke remains unexplained. However, if as has been postulated, structurally higher levels are encountered as one proceeds eastwards, it is necessary to conclude that the second (salic) magma batch became compositionally differentiated prior to its consolidation. If alkalis were able to selectively migrate upwards, a compositionally stratified magma body would have resulted, with phonolitic (foyaite) upper levels grading downwards into trachytic (augite-syenitic) lower levels.

A detailed analysis of a stratified magma body, grading downwards from a phonolitic top to more primitive compositions, has recently been pre-

sented from evidence at Laacher See, Germany (Wörner and Schminke, 1984). Possibly the 'pipe structures' in the OGDC augite-syenite (fig. 3) may relate to the mechanism by which lower density liquid residues may have ascended to higher levels in the intrusion.

Stephenson (1972) presented evidence for serial emplacement of the several units of the South Qôroq foyaitic complex from an originally stratified magma body tapped from the top downwards. Other evidence for comparable zoned Gardar magma chambers has been given by Bridgwater (1967) and Stephenson and Upton (1982). The OGDC central-group may represent the products of such a compositionally zoned magma body which solidified by crystallization from the walls inwards.

The apparent absence of basic border-group rocks from the OGDC sector, immediately east of the Central Complex is also more readily explained by reversion to the concept of a composite intrusion. A model outlined by Upton (1974) for the evolutionary sequence (a) dilational basic dyke, (b) composite dyke production by axial emplacement of salic magma, (c) advance laterally and upwards of the salic magma through the initial confining sheath of basic rocks by stoping, and (d) ultimate production of an annular salic complex by ring-faulting and/or spalling of roof slices, could be applied to many of the features exhibited by the OGDC and the South Qôroq Complex.

### Summary and conclusions

(i) The OGDC is the earliest manifestation of late-Gardar magmatism in the Tugtutôq-Ilimausaq region and was intruded at  $1154 \pm 16$  Ma. The possibility of contemporaneity with either the South Qôroq or Igdlertfigssalik Complexes, some 50 km to the E. of it, cannot be discounted.

(ii) The OGDC is probably a composite intrusion resulting from intrusion of (a) alkali olivine-basalt and then (b) basic trachyte (or benmoreite?) magma.

(iii) The two magma components were cogenetic with the later component related to the basalt by crystal fractionation of olivine, plagioclase, apatite, and opaque oxides.

(iv) The basaltic magma was anhydrous, highly reduced, with a F/Cl ratio > 10. The P, Ti, Ba, and Sr contents are so high as to suggest that enrichment in these elements was a characteristic of the primary magma.

(v) The initial  $^{87}\text{Sr}/^{86}\text{Sr}$  ratio of 0.70326 (cf. 0.70297 for the YGDC, Patchett *et al.*, 1976) suggests minimal contamination by old continental crust. This conclusion is compatible with the style

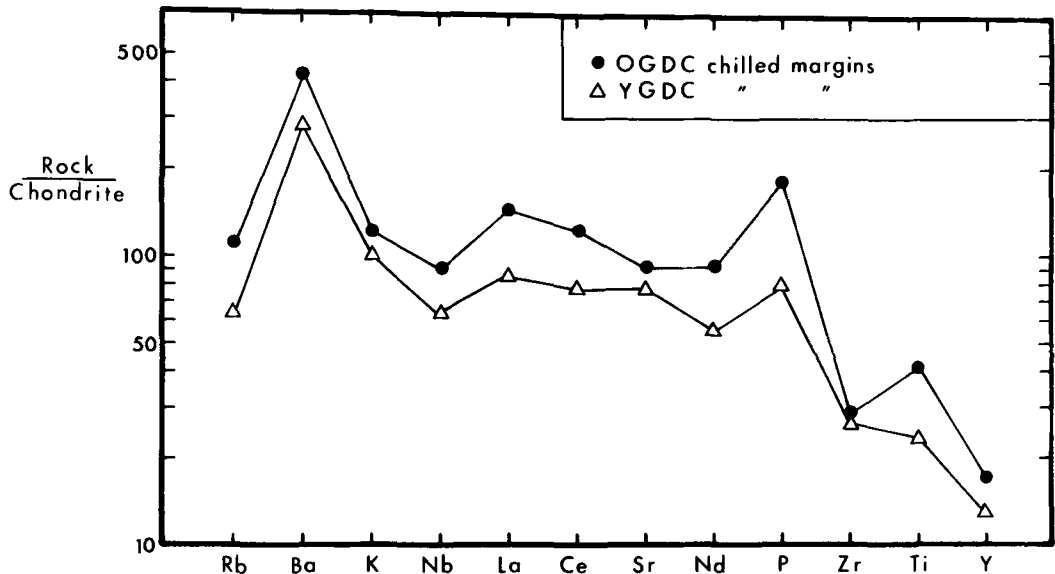


FIG. 17. Chondrite-normalized incompatible element patterns for mean compositions of (a) OGDC chilled margins (closed circles) and (b) YGDC chilled margins (open triangles).

of intrusion, i.e. introduction of magma into a profound crustal 'tension gash' produced by dilation and left-lateral shear.

(vi) The initial intrusion formed a dyke c.200 m wide in which crystallization occurred from the walls inwards with the most magnesian rocks (olivine-gabbros) represented in the chill and more fractionated syenogabbros in the centre.

(vii) Some of the basic magma was retained at depth and underwent further fractionation to a benmoreitic or trachytic composition. This stage involved abundant removal of (sodic) plagioclase under reducing conditions so that the salic residue was strongly depleted in Sr and  $\text{Eu}^{++}$ .

(viii) A second phase of crustal dilation allowed the dyke to expand by a further 300–400 m as the salic magma intruded the axial zone of the dyke. East of the central complex the salic magma appears to have obliterated the basic border group and the composite character is absent.

(ix) Migration of alkalis and halogens to the higher levels of the benmoreitic-trachytic intrusion gave rise to a differentiated magma column whose upper portion became peralkaline and Si-undersaturated. Whereas the parental basalt magma had had a high F/Cl ratio, preferential fractionation of F into apatite caused progressive lowering of the F/Cl ratio during crystallization of the OGDC with Cl being predominant in late residues.

(x) Crystallization of the salic magma again took place primarily from the walls inwards. Because of

the differentiated nature of the magma column, solidification was completed earlier in the lower portions (producing augite-syenites) than in the upper parts which crystallized as sodalite foyaites.

(xi) Crystallization of even such a relatively small and comparatively rapidly cooled intrusion as the OGDC was complex and involved (a) more than one intrusive pulse, (b) crystal fractionation, and (c) diffusive migration of alkalis and halogens.

(xii) The overall similarity between the salic rocks of the OGDC and the augite-syenites, foyaites, etc. of the Ilimaussaq, and Igaliko Complexes, implies that these too originated from alkali olivine-basalt parent magmas by a combination of crystal fractionation and diffusive processes.

*Acknowledgements.* The initial mapping and sample collecting was generously supported by the Geological Survey of Greenland. We are also grateful to the Royal Society and the Natural Environmental Research Council for field-grants in 1974 and 1980. Early mineralogical work by D.S. was supported by the University College of Swansea. We thank D. James for whole-rock XRF analyses and B. M. Kruszewski for ICPAES REE determinations. A. R. Martin gratefully acknowledges assistance from A. Halliday. Thanks also go to R. Macdonald for field assistance, to P. Hill and C. Begg for help with microprobe analysis, to W. Hamilton and K. Cameron for polished thin-section preparation, and to H. Hooker and M. Wright for preparation of the manuscript. We thank I. Parsons, C. H. Emeleus, R. Macdonald, W. S. Watt, and an anonymous reviewer for comment and constructive

criticism. We are further grateful to the Director of the Geological Survey of Greenland for permission to publish.

## REFERENCES

- Abbey, S. (1980) *Geol. Surv. Can Paper* 80-14.
- Blaxland, A. B., van Breemen, O., Emeleus, C. H., and Anderson, J. G. (1978) *Bull. geol. Soc. Am.* **89**, 231-44.
- Blundell, D. J. (1978) *J. geol. Soc. London*, **135**, 545-54.
- Bridgwater, D. (1967) *Can. J. Earth Sci.* **4**, 995-1014.
- Buddington, A. F., and Lindsley, D. H. (1964) *J. Petrol.* **5**, 310-57.
- Carmichael, I. S. E. (1967) *Contrib. Mineral. Petrol.* **14**, 36-64.
- Chambers, A. D. (1976) *The petrology and geochemistry of the North Qôroq Centre, Igaliko Complex, South Greenland*. Unpubl. Ph.D. thesis, Univ. of Durham.
- Emeleus, C. H., and Upton, B. G. J. (1976) In *Geology of Greenland* (Escher, A., and Watt, W. S., eds.). Copenhagen: The Geological Survey of Greenland, 153-81.
- Gill, R. C. O. (1972) *The geochemistry of the Grønnedal-Ika alkaline complex, South Greenland*. Unpubl. Ph.D. thesis, Univ. of Durham.
- Jones, A. P. (1980) *The Petrology and structure of the Motzfeldt Centre, Igaliko, South Greenland*. Unpubl. Ph.D. thesis, Univ. of Durham.
- (1984) *Mineral. Mag.* **48**, 1-12.
- Larsen, L. M. (1976) *J. Petrol.* **17**, 258-90.
- Leake, B. E. (1978) *Mineral. Mag.* **42**, 533-63.
- Norrish, K., and Hutton, J. T. (1969) *Geochim. Cosmochim. Acta*, **33**, 431-53.
- Parsons, I. (1979) *J. Petrol.* **20**, 653-94.
- Patchett, P. J., Hutchinson, J., Blaxland, A. B., and Upton, B. G. J. (1976) *Bull. geol. Soc. Denmark*, **25**, 79-84.
- Powell, M. (1978) *Lithos*, **11**, 99-120.
- Powell, R., and Powell, M. (1977) *Mineral. Mag.* **41**, 257-63.
- Rock, N. M. S., and Leake, B. E. (1984) *Mineral. Mag.* **48**, 211-27.
- Spencer, K. J., and Lindsley, D. H. (1981) *Am. Mineral.* **66**, 1189-201.
- Stephenson, D. (1972) *Lithos*, **5**, 187-201.
- (1974) *Ibid.* **7**, 35-41.
- (1976) *Bull. Grønlands geol. Unders.* **118**, 55 pp.
- and Upton, B. G. J. (1982) *Mineral. Mag.* **46**, 283-300.
- Stormer, J. C. Jr. (1983) *Am. Mineral.* **68**, 586-94.
- Sun, S. S. (1980) *Phil. Trans. R. Soc. Lond.* **A297**, 409-45.
- Sweatman, T. R., and Long, J. V. P. (1969) *J. Petrol.* **10**, 332-79.
- Thirlwall, M. F. (1979) *The petrochemistry of the British Old Red Sandstone Province*. Unpubl. Ph.D. thesis, Univ. of Edinburgh.
- Upton, B. G. J. (1962) *Bull. Grønlands geol. Unders.* **34** (also *Meddr. Grønland*, **169**, 8) 60 pp.
- (1964a) *Ibid.* **8** (also *Meddr. Grønland*, **169**, 2) 1-47.
- (1964b) *Ibid.* **8** (also *Meddr. Grønland*, **169**, 2) 49-180.
- (1974) In *The Alkaline Rocks* (H. Sørensen, ed.) John Wiley, New York, 221-38.
- and Blundell, D. J. (1978) In *Petrology and Geochemistry of Continental Rifts* (E. R. Neumann and I. B. Ramberg, eds.) Reidel, Dordrecht, 163-72.
- and Thomas, J. E. (1980) *J. Petrol.* **21**, 167-98.
- van Breemen, O., and Upton, B. G. J. (1972) *Bull. geol. Soc. Am.* **83**, 3381-90.
- van Breemen, O., Aftalion, M., and Allaart, J. H. (1974) *Ibid.* **85**, 403-12.
- Walsh, J. N., Buckley, F., and Barker, J. (1981) *Chem. Geol.* **33**, 141-53.
- Wörner, G., and Schminke, H.-U. 9 (1984). *J. Petrol.* **25**, 805-35.

[Manuscript received 29 October 1984;  
revised 11 February 1985]